JOURNAL OF GEOPHYSICAL RESEARCH: SPACE PHYSICS, VOL. 118, 4033–4038, doi:10.1002/jgra.50442, 2013

How to identify reconnecting current sheets in incompressible Hall MHD turbulence

S. Donato,[1] A. Greco,[1] W. H. Matthaeus,[2] S. Servidio,[1] and P. Dmitruk[3]

Received 18 March 2013; revised 27 June 2013; accepted 6 July 2013; published 29 July 2013.

[1] Using high Reynolds number simulations of two-dimensional Hall magnetohydrodynamics (HMHD) turbulence, a statistical association between magnetic discontinuities and magnetic reconnection is demonstrated. We find that sets of discontinuities, identified using the normalized partial variance of vector increments (PVI method), strongly depend on threshold in PVI statistic that is used as an identifying condition and on the strength of the Hall term. The analysis confirms that the Hall term plays an important role in turbulence and it affects the methods employed for detection of reconnecting current sheets. In particular, we found the following: (1) Among all the discontinuities detected by the PVI method, the reconnecting ones are on average thinner. (2) A reduction in size of all discontinuities and of reconnecting current sheets is observed as the threshold θ grows. (3) The average width of the reconnecting current sheets decreases as the strength of the Hall term grows and the ion inertial scale d_i increases with respect to the dissipative scale.

Citation: Donato, S., A. Greco, W. H. Matthaeus, S. Servidio, and P. Dmitruk (2013), How to identify reconnecting current sheets in incompressible Hall MHD turbulence, *J. Geophys. Res. Space Physics*, *118*, 4033–4038, doi:10.1002/jgra.50442.

1. Introduction

[2] Besides turbulence, an ingredient that may accelerate the process of reconnection is the Hall effect. Hall magnetohydrodynamics (HMHD) is an extension of the standard MHD where the ion inertia is retained in Ohm's law. The Hall effect becomes relevant when we intend to describe the plasma dynamics down to length scales of the order or shorter than the *ion inertial length* d_i ($d_i = c/\omega_{pi}$, where c is the speed of light and ω_{pi} is the ion plasma frequency). In other words, for large-scale phenomena, this term is negligible and we recover the standard MHD equations. Generally, the Hall effect is thought to be fundamental for astrophysical plasmas, since it modifies small-scale turbulent activity, producing a departure from MHD predictions [*Dmitruk and Matthaeus*, 2006; *Galtier and Buchlin*, 2007; *Servidio et al.*, 2007]. In particular, it has been proposed that the Hall effect in reconnection causes a catastrophic release of magnetic energy, leading to fast magnetic reconnection onset [*Cassak et al.*, 2005, 2007], with reconnection rates faster than the Sweet-Parker expectation.

[3] In the past years, the role of the ion skin depth d_i on reconnection has been subject of several numerical investigations [*Shay et al.*, 1998; *Ma and Bhattacharjee*, 2001; *Smith et al.*, 2004]. Recently, *Servidio et al.* [2011b] and *Donato et al.* [2012] show that in a two-dimensional HMHD turbulent simulation, higher tails appear in the distributions of reconnection electric fields respect to the MHD case, leading to slightly faster rates on average, but a net increase in the frequency of occurrence of the fastest rates. In those works, it was also shown that Hall effect causes the appearance of longer tails in the distributions of the current density. The current density is an important quantity since it develops small-scale features in both turbulence and in reconnection, so pronounced tails in its distribution may be a signature of more intense small-scale activity. Finally, *Donato et al.* [2012] point out that the Hall term in simulations reduces the thickness of the reconnecting current sheets as it does in analysis of single reconnection sites [*Shay et al*., 1998]. More precisely, on average, the current sheets are both thinner and shorter than in the MHD counterpart. Figure 1 illustrates magnetic field lines together with the diffusion regions from a MHD simulation (blue-shaded map) and HMHD one (red-shaded map) [*Donato et al.*, 2012]. It is clear that the current sheets in the diffusion zones become thinner and shorter when the Hall term is considered. This is reminiscent of the systematic shortening and thinning of current sheets seen in isolated laminar reconnection simulations [*Shay et al.*, 1998].

2. HMHD Turbulence Simulation

[4] The equations of incompressible Hall MHD can be written in terms of Alfvén units, with lengths scaled to L_0, a typical large-scale length, velocities and magnetic fields scaled to the root mean square Alfvén speed C_A, and times

[1]Dipartimento di Fisica, Università della Calabria, Cosenza, Italy.
[2]Bartol Research Institute and Department of Physics and Astronomy, University of Delaware, Newark, Delaware, USA.
[3]Departamento de Física, Facultad de Ciencias Exactas y Naturales, Universidad de Buenos Aires and Instituto de Física de Buenos Aires, CONICET, Buenos Aires, Argentina.

Corresponding author: A. Greco, Dipartimento di Fisica, Universita della Calabria, IT-87036 Cosenza, Italy. (greco@fis.unical.it)

2169-9380/13/10.1002/jgra.50442

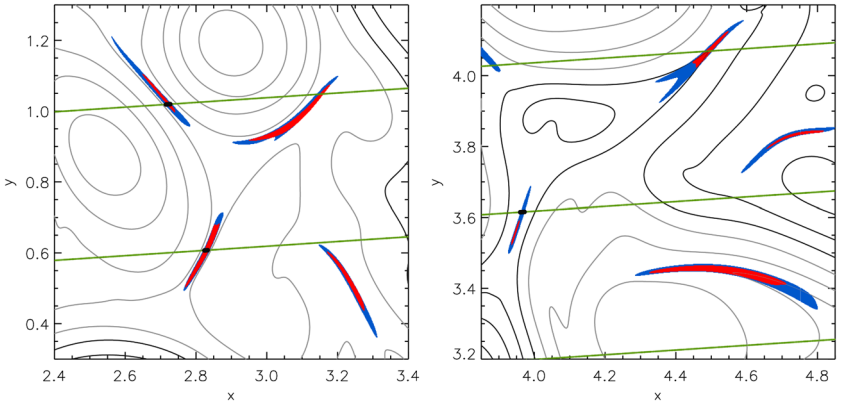

Figure 1. Magnetic field lines together with the diffusion regions in two subregions of the simulation box from a MHD simulation (blue-shaded map) and from an HMHD one (red-shaded map). Green line is one-dimensional path s, and black bullets correspond to discontinuities detected by the partial variance of vector increments (PVI) method with $\theta = 7$.

scaled to a characteristic Alfvén time $\tau_A = L_0/C_A$. In 2.5-D (two dimensions in the physical space for three-dimensional components), the equations are

$$\frac{\partial \boldsymbol{v}}{\partial t} = -(\boldsymbol{v}\cdot\nabla)\boldsymbol{v} - \nabla P + \boldsymbol{j}\times\boldsymbol{b} + R_v^{-1}\nabla^2\boldsymbol{v} \quad (1)$$

$$\frac{\partial \boldsymbol{b}}{\partial t} = \nabla\times[(\boldsymbol{v} - \epsilon_H\boldsymbol{j})\times\boldsymbol{b}] + R_\mu^{-1}\nabla^2\boldsymbol{b} \quad (2)$$

where $\boldsymbol{v}$ is the velocity field and $\boldsymbol{b}$ is the magnetic field. Both fields can be decomposed into perpendicular (in-plane) and parallel (out-of-plane, along z) components, namely, $\boldsymbol{b} = (\boldsymbol{b}_\perp, b_z)$ and $\boldsymbol{v} = (\boldsymbol{v}_\perp, v_z)$. The in-plane magnetic field is $\boldsymbol{b}_\perp = \nabla a \times \hat{z}$, where a is the magnetic potential. No external mean field has been imposed because, in order to have a dynamical effect of the out-of-plane field, one would require compressibility (see e.g., *Dmitruk and Matthaeus* [2009] for the 3-D case). In equations (1) and (2), $\boldsymbol{j} = \nabla\times\boldsymbol{b}$ is the current density and P is the pressure that stems from the solenoidal condition $\nabla\cdot\boldsymbol{v} = 0$. The parameters R_μ and R_ν are the magnetic and the kinetic Reynolds numbers, respectively. The coefficient $\epsilon_H = d_i/L_0$ is the Hall parameter that measures the strength of the Hall term relative to effects that depend on the energy-containing scale. Note that for $\epsilon_H \to 0$, equations (1) and (2) reduce to MHD. Generally speaking, the Hall term becomes a significant factor at wave numbers k such that $kL_0\epsilon_H = kd_i \sim 1$. Just as the reciprocal Reynolds numbers $1/R_\nu$ and $1/R_\mu$ provide a measure of the strength of dissipation, the dimensionless parameter ϵ_H in equation (2) determines the strength of Hall modifications to the Ohm's law, including dispersion.

[5] The above equations (1) and (2) are solved in doubly periodic (x, y) Cartesian geometry, with a box size of $2\pi L_0$, using 4096^2 grid points, and with $R_\mu = R_\nu = 1700$. The maximum resolved wave number is $k_{\max} = 4096/3 \sim 1365$. We use a well-tested and accurate pseudo-spectral code, fully dealiased with a 2/3 rule. More details can be found in *Servidio et al.* [2010], *Servidio et al.* [2011a], and *Donato et al.* [2012]. Considering a representation of the fields in the Fourier space, the energy is initially concentrated in a shell with $4 \le k \le 10$ (wave numbers k in units of $1/L_0$) with mean value E=(1/2)$\langle|\mathbf{v}|^2 + |\mathbf{b}|^2\rangle \simeq 1$, where $\langle\ldots\rangle$ indicates a volume average. Random phases are employed for the initial Fourier coefficients. Initial velocity and magnetic field fluctuations are chosen to have equal energies.

[6] We chose three different values for the Hall parameter, that is, $\epsilon_H = 1/400, 1/100, 1/50$, but we mostly discuss results with $\epsilon_H = 1/100$ where the Hall effect is already relevant on the entire reconnection process [*Donato et al.*, 2012] and the reconnecting current sheets have an appreciable dimension, as shown in the following section.

[7] In the solar wind near 1 AU $\epsilon_H \sim 10^{-4}$ and in the lower solar corona $\epsilon_H \sim 10^{-5}$, while in the magnetosphere environment, ϵ_H is of the order of 0.03–0.1 (see, e.g., parameters in *Axford and McKenzie* [1997]). In the first two cases, the Hall scale is much smaller than the typical energy-containing scale, at which its effects are negligible. On the other hand, the Hall term contributes significantly at small scales $\le d_i$.

[8] We considered the system at a fixed time $t \sim 0.5\tau_A$ of the turbulent evolution, at which time the mean square current density $\langle j_z^2\rangle$ is very near to its peak value. At this time, in fact, the peak of small-scale turbulent activity is achieved, the resulting turbulence correlation length is $\lambda_C = 0.179$, and the dissipation scale is $\lambda_d = 0.0053$. Coherent structures are a familiar feature of fully developed turbulence. They can be identified as magnetic islands that differ in size and energy. Between these interacting islands, the perpendicular (out-of-plane) component of the current density j_z becomes very high.

[9] We employed a cellular automata scheme to identify the diffusion regions [*Servidio et al.*, 2010; *Servidio et al.*, 2011a] . Briefly, the main steps are the following: (i) Identify critical points at $\boldsymbol{x}^*$, where $\nabla a = 0$. (ii) From the analysis of the Hessian matrix of a, X points are found (saddle points of the potential a). (iii) These points are characterized with their respective width δ, elongation ℓ, and the respective reconnection electric field $E_\times = -da/dt$. (iv) A threshold is set by the value of the current at the positions $\pm\delta/2$ for each critical point. Then a cellular automaton-like method is used to propagate a label for that diffusion region to nearby points satisfying the selected condition. (v) An index n is used to identify each island. With the above procedure, the shape and the position of each diffusion region are defined. This procedure was performed for the strongest reconnection

sites, for which $\ell/\delta > 10$ holds. (see *Servidio et al.* [2010] for more details).

[10] In order to quantify the differences between MHD and HMHD turbulence, *Donato et al.* [2012] computed the power spectra for $\boldsymbol{b}_\perp$ (in-plane components) for four runs of MHD and HMHD which start with the same initial conditions. The main difference between the runs can be noticed at small scales, and it is attributed to the presence of Hall corrections to the Ohm's law [*Servidio et al.*, 2007]. For the same runs, the probability distribution functions (PDFs) of j_z (out-of-plane component) and of the reconnection electric field $E_\times$ displays a very similar core, but in the HMHD cases, the tails are more pronounced. This suggests that dispersive effects cause an enhancement of the small-scale activity and indicate that the Hall term slightly accelerates reconnection, with very few events characterized by reconnection electric fields faster than laminar regimes.

3. Discontinuities and Reconnection Events in HMHD Turbulence

[11] In *Servidio et al.* [2011a], a statistical association between tangential discontinuities (TDs) and magnetic reconnection has been demonstrated. Methods employed in previous studies on discontinuities and reconnection in turbulence were used to identify sets of possible reconnection events along a one-dimensional path through a 2-D MHD turbulent field, emulating experimental sampling by a single detector in a high-speed flow. It was found that sets of strong discontinuities, identified using the normalized PVI, include an increasing fraction of reconnection events as the threshold in PVI statistic that is used as an identification criterion of structures grows. Magnetic discontinuities become almost purely reconnection events for high thresholds, with values generally higher than 6 standard deviations. In the present work, we extend the investigation carried out in *Servidio et al.* [2011a] to the HMHD case.

[12] Following *Servidio et al.* [2011a], we describe rapid changes in the magnetic field, looking at the increments $\Delta\mathbf{b}(s, \Delta s) = \mathbf{b}(s + \Delta s) - \mathbf{b}(s)$, calculated along a 1-D path s in the simulation box on a spatial separation or lag Δs. In the Hall case, we consider $\mathbf{b}$ as the perpendicular magnetic field, namely b_x and b_y, because we suppose that the most relevant variations when crossing a current sheet are in the magnetic vector components lying in the plane. Employing only the sequence of magnetic increments, we compute the normalized magnitude

$$\Im = \frac{|\Delta\mathbf{b}(s, \Delta s)|}{\sqrt{\langle|\Delta\mathbf{b}(s, \Delta s)|^2\rangle}}, \tag{3}$$

where $\langle\bullet\rangle$ denotes a spatial average over the total length of the data set, and Δs is the spatial lag in the definition of magnetic field increments. The above quantity has been called the PVI [*Greco et al.*, 2008]. The method is sensitive to directional changes, magnitude changes, and any form of sharp gradient in the vector magnetic field. The PVI quantity is defined in order to relate it easily to statistics associated with intermittency, and it is not biased toward a particular type of discontinuity (directional, tangential, and rotational discontinuities and shocks) or other structures. These properties have been discussed in earlier papers [*Greco et al.*, 2008; *Greco et al.*, 2009a, 2009b]. For brevity, we will sometimes refer to the identified discontinuities as "TDs", solely because this is a familiar type of structure found in these simulations.

Table 1. Performance of PVI Technique and Reconnection Events Identification[a]

θ	# ITD	# IRS	E (%)	G (%)	δ'/λ_d (*ITD*)	δ'/λ_d (*IRS*)
1	365	25	100	6.8	3.37	2.20
2	136	25	100	18.4	3.1	2.20
3	81	24	96	29.6	2.86	2.17
4	54	23	92	42.5	2.69	2.13
5	34	20	80	58.8	2.31	2.05
6	22	16	64	72.7	2.24	2.05
7	19	14	56	73.7	2.14	1.90
8	13	10	40	76.9	2.05	1.70

[a]First column: Threshold θ imposed on PVI. Second column: #*ITD*, number of discontinuities identified by the method. Third column: #*IRS*, number of reconnection sites found by the method. Fourth column: E = #*IRS*/#*RS*, the relative efficiency of the method. Fifth column: G = #*IRS*/#*ITD*, the relative goodness of the method. Sixth column: average optimized width computed for all the TDs normalized to the dissipation length. Seventh column: average optimized width computed for the TDs that are RSs normalized to the dissipation length.

[13] This technique has been subjected to numerous tests. The interested reader is referred to the literature for quantitative comparison of performance of the PVI method relative to classical discontinuity identification methods [*Greco et al*., 2008] and for comparison of waiting times distributions in MHD simulations and in Advanced Composition Explorer spacecraft (ACE) magnetic field data [*Greco et al.*, 2009a, 2009b].

[14] Since we expect that the strongest current sheets are on scales of the dissipation length, for this simulation, we choose a small-scale lag, $\Delta s \simeq 0.3\lambda_d$. The corresponding PVI time series is bursty (not shown), suggesting the presence of sharp gradients and localized coherent structures in the magnetic field that represent the spatial intermittency of turbulence. These events may correspond to what are qualitatively called "tangential discontinuities" and, possibly, to reconnection events.

4. Effect of Threshold and Hall Parameter on the Identification of Reconnecting Current Sheets

[15] While examining the values of PVI defined by equation (3) continuously along the trajectory (increasing values of s), we select points as events when $\Im > \theta$, where the value θ is called *threshold*. This condition is based on the idea that large isolated values of PVI represent a signature of intermittent structures. In order to identify candidate reconnection sites among them, we follow the same procedure as in *Servidio et al.* [2011a] to count how many of the identified TDs are also reconnection sites. In summary, for a given threshold θ of PVI, there will be a set of identified TDs (a set *ITD* with number of elements #*ITD*); there will be a subset of these discontinuities that are Identified Reconnection Sites (a set *IRS* with number of elements #*IRS*). There will also be a complementary set of identified TDs that are not RSs, numbering #*ITD* – #*IRS*, and reconnection regions lying along the trajectory that are not captured at all by the technique, numbering #*RS* – #*IRS*, where #*RS* is the total

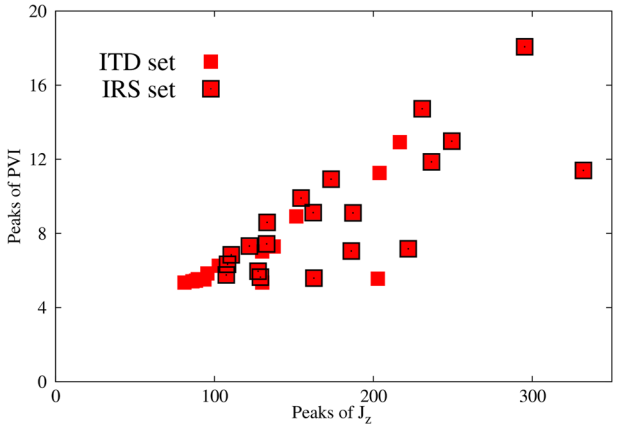

Figure 2. Scatterplot of the peaks of PVI signal and peaks of the current density j_z encountered across the ITD set (red squares) and across the IRS set (red squares with black border), for $\theta = 5$ and $\epsilon_H = 0.01$.

number of strong reconnection site encounters found along the trajectory. *#IRS* events are characterized by a rotation of the magnetic field. In the HMHD case, a third component of the magnetic field appears, that is b_z, which exhibits the quadrupolar signature of Hall effect in turbulent reconnection (not shown). None of these features was present at the initial time in which the electric current is not concentrated but rather is randomly distributed by construction.

[16] The parameters of different PVI-based algorithms are listed in Table 1. It can be seen that for higher values of θ, an increasing fraction of the identified TDs corresponds to a reconnection site. That is, the goodness ratio $G = \#IRS/\#ITD$ increases as the threshold θ gets larger values. Note that 25 strong reconnection sites actually lie along the trajectory. We found among the 365 TDs with $\theta = 1$ that only 25 are reconnecting current sheets. In this sense, a lower threshold such as $\theta = 1$ is very effective—*all* possible reconnection sites are found. There are, however, a large number of false positives (365 – 25 are simply current sheets with a high-stressed magnetic field). In contrast, a large threshold value ($\theta = 7$ or $\theta = 8$) has very few false positives but identifies at most 40% of the actual number of strong reconnection sites that are known to lie along the trajectory. In this case the goodness of the technique, proportional to the ratio between the total number of identified tangential discontinuities and the known reconnection sites, is of the order of 77%. This value is slightly less respect to the one obtained in MHD case (see Table I in *Servidio et al.* [2011a]). This maybe because in that case at least one point of an identified candidate discontinuity overlapped with one point of the identified reconnection region, so that the event was counted as a "success", in the Hall case the same discontinuity along the path s does not intercept the diffusion region because the latter has become shorter and thinner, and the event is counted as a false positive. In the left panel of Figure 1, two examples of discontinuities (black bullets) along the one-dimensional path s (green line) intercept a diffusion region in both MHD and Hall cases. In the right panel, the single discontinuity corresponds to a reconnection region only in the MHD case.

[17] In order to estimate the width of the TDs, we make use of the field $W(s, \Delta s) = |\Delta_2 \boldsymbol{b}|/\langle|\Delta_2 \boldsymbol{b}|^2\rangle$, where $|\Delta_2 b_j| = b_j(s - \Delta s) - 2b_j(s) + b_j(s + \Delta s)$, with $j = x, y$, and $\Delta s = 0.3\lambda_d$, as in the definition of the PVI series. Note that the PVI series for small lags becomes proportional to a normalized first derivative of the magnetic field (cf. equation (3)). Analogously, the W-field becomes proportional to a second derivative, in the sense of a finite difference formula approximation to a Taylor series expansion. We now recall that the current sheets associated with reconnection events in turbulence are well approximated by hyperbolic functions [*Servidio et al.*, 2010]. In this case we can make an approximation that $\Im \sim sech^2[(s - s_0)/\delta]$, where s_0 corresponds to the center of discontinuity, and its second derivative (W) has two peaks at $\sim \pm\delta/2$. Once each reconnection site has been identified and "expanded" using the above technique, we can determine the direction or orientation of each TD. Using the assumption that the structures are one dimensional, the minimum variance analysis technique [*Sonnerup and Cahill*, 1967] allows us to determine the normal vector $\hat{\mathbf{n}}$ to the discontinuity surface if single point measurements are used. For each TD identified with the PVI method, and for which we have determined a width δ, we compute a refined estimate of the width, namely $\delta' = \cos(\alpha)\delta$, where α is the angle between $\hat{\mathbf{n}}$ and the trajectory direction $\hat{\mathbf{s}}$ (for more details, see *Servidio et al.* [2011a]).

[18] Table 1 contains the values of δ' averaged over all the discontinuities detected by the PVI method (*ITD* set), at different thresholds θ. In the same table, we also report the values of δ' only averaged over the reconnecting current sheets (*IRS* set). It is noticeable that when the false positives (nonreconnecting current sheets) are left out from the computation of the average width, the latter is smaller, meaning that the effective reconnecting discontinuities are on average thinner. At the same time, δ' decreases with the growth of θ in both set, meaning a reduction in size of the most intermittent current sheets.

[19] We also determined the width d of each reconnection site using the method of *Servidio et al.* [2010]. A Hessian analysis of the magnetic potential gives a direction associated with the maximum eigenvalue. In that direction, a fit is carried out using a hyperbolic function (e.g., *sech*), providing a width for each current sheet. For the average over the entire simulation, we obtained that $\langle d \rangle = 8.49 \times 10^{-3}$. This is in good agreement with 9.04×10^{-3}, the average size of the most intermittent reconnecting current sheets when $\theta = 8$. We point out that the above value for δ' is less than $2\lambda_d$. In the MHD case, we obtained that the corresponding δ' was about $3\lambda_d$ [*Servidio et al.*, 2011a].

Table 2. Features of the Reconnecting Current Sheets for Different Values of the Hall Parameter[a]

ϵ_H	d_i/λ_d	# IRS	δ'/λ_d (*IRS* set)	$\langle d\rangle/\lambda_d$ (from 2-D sim)
MHD	0	13	2.74	2.78
0.0025	0.5	14	2.63	2.63
0.01	2	10	1.70	1.60
0.02	3.6	7	1.47	0.99

[a]First column: Hall parameter $\epsilon_H = d_i/L_0$. Second column: the ratio between the ion skin depth and the dissipation scale. Third column: *#IRS*, number of reconnection sites found by the method. Fourth column: optimized width δ' averaged over IRS set at $\theta = 8$, normalized to the dissipation length. Fifth column: width $\langle d\rangle$ computed from the 2-D simulation normalized to the dissipation length. The values of the dissipation lengths for different ϵ_H are listed in *Donato et al.* [2012]

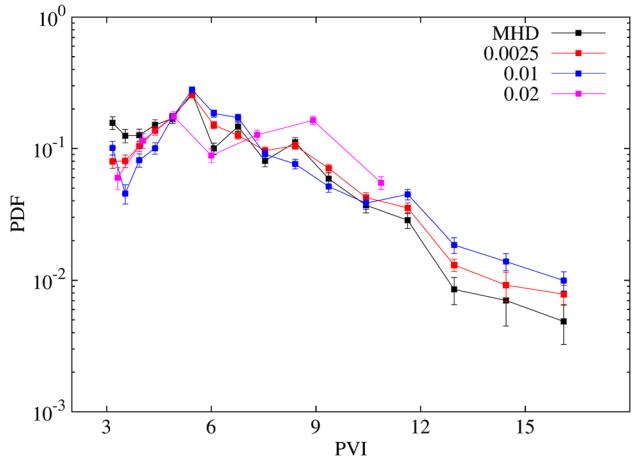

Figure 3. PDFs of PVI signal inside the reconnecting current sheets (*IRS* set), for $\epsilon_H = 0$, 0.0025, 0.01 and 0.02.

[20] Finally, we show in Figure 2 the scatterplot of the peaks of PVI signal versus the peaks of the current density j_z when crossing all the identified TDs (*ITD* set) and the reconnecting current sheets (*IRS* set), at $\theta = 5$ (we choose this case because we have a larger number of points, but we expect similar results using other values of the threshold). Points tend to lie along a line and the linear correlation coefficient r is 0.8 for *ITD* points (and 0.77 for *IRS* ones), meaning that larger peaks of current density correspond statistically to larger peaks in PVI. For this reason, the PVI method is able to describe and identify the current density enhancements and thus, the strong magnetic gradients [*Greco et al.*, 2008, 2009a]. From the plot, it is clear that when selecting the reconnection zones among the ITD set, the lower peaks of PVI and j_z are excluded. Indeed, the reconnecting current sheets have, in average, the highest peaks of PVI and current density [*Donato et al.*, 2012].

[21] In order to check the effectiveness of the PVI technique in the detection and description of current sheets when they become narrower, due to the presence of the Hall term, we carried out a parametric study using other values of ϵ_H. Table 2 shows the values of δ' averaged over the reconnecting current sheets (*IRS* set) (at $\theta = 8$) and $\langle d \rangle$ computed from the 2-D simulation for $\epsilon_H = d_i/L_0 = 0$, 0.0025, 0.01 and 0.02 [*Donato et al.*, 2012]. In the same table, we report the ratio d_i/λ_d. It is evident that the average width of the reconnecting current sheets decreases as ϵ_H grows and d_i increases with respect to the dissipative scale, confirming that the Hall term contributes significantly to the dynamics of small-scale turbulence, making current sheets thinner. There is one more interesting feature: the agreement between the columns of δ' and $\langle d \rangle$ is remarkable as long as $\epsilon_H \leq 0.01$. For larger values, the difference becomes more important and the average width of the diffusion regions is smaller than that computed for the TDs detected by the PVI method.

[22] To get more insight, Figure 3 illustrates the PDFs of PVI inside the reconnecting current sheets when using different Hall parameters. The core of the distributions is very similar for all the simulations, but, in the HMHD cases, the tails are more pronounced, which in turn means that j_z has a greater probability to get larger values, revealing more frequently occurring explosive reconnection events than in the MHD counterpart. We point out that the statistics are most poor in the case $\epsilon_H = 0.02$. It is due to the fact that the *#IRS* is small, as shown in Table 2.

5. Conclusions

[23] We performed a parametric study on the influence of the Hall term in the detection of reconnecting current sheets identified by the PVI method. Using high Reynolds number simulations of two-dimensional HMHD turbulence, a statistical association between tangential discontinuities and magnetic reconnection is demonstrated. We found that only a portion of discontinuities are reconnection sites, and this number strongly depends on threshold in the PVI statistic and on the strength of the Hall term. Main results are the following:

[24] 1. Among all the discontinuities detected by the PVI method, the reconnecting ones are on average thinner.

[25] 2. A reduction in size of all discontinuities and of reconnecting current sheets is observed as the threshold θ grows.

[26] 3. The average width of the reconnecting current sheets decreases as ϵ_H grows and d_i increases with respect to the dissipative scale.

[27] The employed values of the Hall parameter, that is, $\epsilon_H = 1/400, 1/100, 1/50$, reflect different physical situations that can occur: when $\epsilon_H = 1/400$ (very close to the MHD case), the ion skin depth is smaller than the dissipation scale and the Hall term does not strongly influence the dynamics of the turbulent cascade. In the other two cases, the ion skin depth is very close, or larger than the dissipation scale so that the Hall term becomes important and it is interesting that the dissipation scale is the typical size of the TDs in which we are interested. The values $\epsilon_H = 1/400, 1/100, 1/50$ are actually far from those which characterize the solar wind but are close to those of the magnetospheric environment. For this reason the results obtained from these runs may be a reasonable starting point, designed as theoretical background for missions such as National Aeronautics and Space Administration's (NASA) Magnetosphere Multiscale designed for studying the microphysics of three fundamental plasma processes: magnetic reconnection, energetic particle acceleration, and turbulence.

[28] We close by noting that even if PVI technique misses some very thin reconnecting regions, it identifies regions very close to them. This could be even more useful if we think that a rich variety of physical processes, as, e.g., accelerated particles, reconnection exhaust regions and Alfvèn disturbances, occur away from the reconnection site [*Gosling and Szabo*, 2008]. It may be possible using this approach to uncover numerous reconnection events and regions around them that might be present in the solar wind and magnetospheric environment and testing against reported identifications using other methods.

[29] **Acknowledgments.** This research was supported in part by NASA through the Heliosphysics Theory Program NNX11AJ44G, by the MMS Theory and Modeling Team, and also by the NSF Solar Terrestrial and SHINE programs, AGS-1063439 and -1156094, POR Calabria FSE 2007/2013, and EU FP7 Marie Curie People project "Turboplasmas".

[30] Philippa Browning thanks the reviewers for their assistance in evaluating this paper.

References

Axford, W. I., and J. F. McKenzie (1997), The Solar Wind, in *Cosmic Winds and the Heliosphere*, edited by J.R. Jokipii, C.P. Sonett, and M.S Giampapa, Univ. of Arizona, Tucson, Ariz.

Cassak, P. A., J. F. Drake, and B. Eckhardt (2007), Onset of fast magnetic reconnection, *Phys. Rev. Lett.*, *98*, 215001.

Cassak, P. A., M. A. Shay, and J. F. Drake (2005), Catastrophe model for fast magnetic reconnection onset, *Phys. Rev. Lett.*, *95*, 235002.

Dmitruk, P., and W. H. Matthaeus (2006), Structure of the electromagnetic field in three-dimensional Hall magnetohydrodynamic turbulence, *Phys. Plasmas*, *13*, 042307.

Dmitruk, P., and W. H. Matthaeus (2009), Waves and turbulence in magnetohydrodynamic direct numerical simulations, *Phys. Plasmas*, *16*, 062304.

Donato, S., S. Servidio, P. Dmitruk, V. Carbone, M. A. Shay, P. A. Cassak, and W. H. Matthaeus (2012), Reconnection events in two-dimensional Hall magnetohydrodynamic turbulence, *Phys. Plasmas*, *19*, 092307.

Galtier, S., and E. Buchlin (2007), Multiscale Hall-magnetohydrodynamic turbulence in the solar wind, *Astrophys. J.*, *656*, 560.

Gosling, J. T., and A. Szabo (2008), Bifurcated current sheets produced by magnetic reconnection in the solar wind, *J. Geophys. Res.*, *113*, A10103, doi:10.1029/2008JA013473.

Greco, A., P. Chuychai, W. H. Matthaeus, S. Servidio, and P. Dmitruk (2008), Intermittent MHD structures and classical discontinuities, *Geophys. Res. Lett.*, *35*, L19111, doi:10.1029/2008GL035454.

Greco, A., W. H. Matthaeus, S. Servidio, P. Chuychai, and P. Dmitruk (2009a), Statistical analysis of discontinuities in solar wind ACE data and comparison with intermittent MHD turbulence, *Astrophys. J.*, *691*, L111.

Greco, A., W. H. Matthaeus, S. Servidio, and P. Dmitruk (2009b), Waiting-time distributions of magnetic discontinuities: Clustering or Poisson process? *Phys. Rev. E*, *80*, 046401.

Ma, Z. W., and A. Bhattacharjee (2001), Hall magnetohydrodynamic reconnection: The Geospace Environment Modeling challenge, *J. Geophys. Res.*, *106*, 3773.

Servidio, S., V. Carbone, L. Primavera, P. Veltri, and K. Stasiewicz (2007), Compressible turbulence in Hall magnetohydrodynamics, *Planet. Space Sci.*, *55*, 2239.

Servidio, S., W. H. Matthaeus, M. A. Shay, P. Dmitruk, P. A. Cassak, and M. Wan (2010), Statistics of magnetic reconnection in two-dimensional magnetohydrodynamic turbulence, *Phys. Plasmas*, *17*, 032315.

Servidio, S., A. Greco, W. H. Matthaeus, K. T. Osman, and P. Dmitruk (2011a), Statistical association of discontinuities and reconnection in magnetohydrodynamic turbulence, *J. Geophys. Res.*, *116*, A09102, doi:10.1029/2011JA016569.

Servidio, S., P. Dmitruk, A. Greco, M. Wan, S. Donato, P. A. Cassak, M. A. Shay, V. Carbone, and W. H. Matthaeus (2011b), Magnetic reconnection as an element of turbulence, *Nonlin. Proc. Geophys.*, *18*, 675.

Shay, M. A., J. F. Drake, R. E. Denton, and D. Biskamp (1998), Structure of the dissipation region during collisionless magnetic reconnection, *J. Geophys. Res.*, *103*, 9165.

Smith, D., S. Ghosh, P. Dmitruk, and W. H. Matthaeus (2004), Hall and turbulence effects on magnetic reconnection, *Geophys. Res. Lett.*, *31*, L02805, doi:10.1029/2003GL018689.

Sonnerup, B. U. O., and L. J. Cahill (1967), Magnetopause structure and attitude from Explorer 12 observations, *J. Geophys. Res.*, *72*, 171.